Journal of Zhejiang University-SCIENCE B (Biomedicine & Biotechnology) *2021 22(6):450-461*
www.jzus.zju.edu.cn; www.springer.com/journal/11585
E-mail: jzus_b@zju.edu.cn

Research Article
https://doi.org/10.1631/jzus.B2000683

Cytocompatible cellulose nanofibers from invasive plant species *Agave americana* L. and *Ricinus communis* L.: a renewable green source of highly crystalline nanocellulose

Olga L. EVDOKIMOVA[1], Carla S. ALVES[1], Radenka M. KRSMANOVIĆ WHIFFEN[1,2], Zaida ORTEGA[3]✉, Helena TOMÁS[1], João RODRIGUES[1,4]✉

[1]*CQM–Centro de Química da Madeira, MMRG, Universidade da Madeira, Campus Universitário da Penteada, 9020-105 Funchal, Portugal*
[2]*Faculty of Polytechnics, University of Donja Gorica, Oktoih 1, 81000 Podgorica, Montenegro*
[3]*Departamento de Ingeniería de Procesos, Universidad de Las Palmas de Gran Canaria, 35017 Las Palmas de Gran Canaria, Las Palmas, Spain*
[4]*School of Materials Science and Engineering/Center for Nano Energy Materials, Northwestern Polytechnical University, Xi'an 710072, China*

Abstract: In this study, the fibers of invasive species *Agave americana* L. and *Ricinus communis* L. were successfully used for the first time as new sources to produce cytocompatible and highly crystalline cellulose nanofibers. Cellulose nanofibers were obtained by two methods, based on either alkaline or acid hydrolysis. The morphology, chemical composition, and crystallinity of the obtained materials were characterized by scanning electron microscopy (SEM) together with energy-dispersive X-ray spectroscopy (EDX), dynamic light scattering (DLS), X-ray diffraction (XRD), and Fourier transform infrared (FTIR) spectroscopy. The crystallinity indexes (CIs) of the cellulose nanofibers extracted from *A. americana* and *R. communis* were very high (94.1% and 92.7%, respectively). Biological studies evaluating the cytotoxic effects of the prepared cellulose nanofibers on human embryonic kidney 293T (HEK293T) cells were also performed. The nanofibers obtained using the two different extraction methods were all shown to be cytocompatible in the concentration range assayed (i.e., 0–500 μg/mL). Our results showed that the nanocellulose extracted from *A. americana* and *R. communis* fibers has high potential as a new renewable green source of highly crystalline cellulose-based cytocompatible nanomaterials for biomedical applications.

Key words: Nanofiber; Nanocellulose; *Agave americana* L.; *Ricinus communis* L.; Crystallinity; Invasive species; Biomedical application

1 Introduction

The increasing number of invasive species worldwide is considered a global environmental and economic problem and a major threat to biodiversity (Charles and Dukes, 2007). These invasive species are damaging the native fauna and flora of ecosystems, leading to severe threats to local biodiversity, agricultural and forest production, and ultimately to human health (Mooney and Hobbs, 2000; Crowl et al., 2008).

✉ Zaida ORTEGA, zaida.ortega@ulpgc.es
João RODRIGUES, joaor@uma.pt; joaoc@staff.uma.pt
Zaida ORTEGA, https://orcid.org/0000-0002-7112-1067
João RODRIGUES, https://orcid.org/0000-0003-4552-1953

Received Oct. 24, 2020; Revision accepted Jan. 8, 2021;
Crosschecked Apr. 12, 2021

Invasive plant species can be exploited as a cheap and widely available renewable source of cellulosic fibers (Satyanarayana et al., 2013; Sun et al., 2020). At present, the exploitation of various non-traditional sources of cellulose (such as annual plants, vegetables, weeds, residues from crops such as wheat/vine stems, corn grain/cobs, sugarcane bagasse, and marine residues) is gaining more importance as a way to reduce the high consumption of natural fibers and to find new strategies for their potential application and valorization (Aguir and M'Henni, 2006; Fiserova et al., 2006; Abrantes et al., 2007; Khiari et al., 2011; Ridzuan et al., 2016). For instance, Abrantes et al. (2007) used annually harvested non-wood fibers from *Cynara cardunculus* L. (cardoon) for paper and paperboard production. Maheswari et al. (2012) extracted cellulose microfibrils from the agricultural residue of coconut palm leaf sheaths. Another research group (Fiore et al.,

2014) studied the possibility of using an invasive plant, *Arundo donax* L., as a source of reinforcement fibers in polymer composites. Our team recently explored the use of pure *Agave americana* L. fibers for reinforcement in polymer composites (Ortega et al., 2019).

Within the past decade, nanoscale cellulose has demonstrated great potential in the biomedical field, namely, in drug delivery, tissue engineering, cartilage replacements, medical implants, skin wound dressings, bioimaging, and biosensing (Lin and Dufresne, 2014; Guise and Fangueiro, 2016; Kargarzadeh et al., 2017; Mishra et al., 2018; Xu et al., 2018). Nanocellulose has been exploited as a biomaterial for three-dimensional (3D) printing to design drug delivery devices with the desired drug release profile for personalized therapy (Yu et al., 2009; Sandler and Preis, 2016). Lately, nanocellulose has been increasingly utilized as 3D scaffolds in liver tissue engineering, adipose tissue engineering, and vascular tissue engineering (Bacakova et al., 2019). Rees et al. (2015) explored the application of nanocellulose as a bioink for possible use as a wound-dressing material. Åhlén et al. (2018) developed contact lenses based on cellulose-nanocrystal-reinforced polyvinyl alcohol that could be used for controlled ocular drug delivery. Bacterial nanocellulose has been applied as a new patch for the repair of congenital heart defects (Lang et al., 2015). Another interesting use of nanocellulose was reported by Wang et al. (2016). They obtained biocomposites of nanofibrillated cellulose for dressing materials in an emerging concept of Cu-containing wound healing dressings.

Numerous studies have demonstrated the possibility of obtaining cellulose nanofibers, nanocrystals, or nanofibrils from non-conventional cellulose resources (Oun and Rhim, 2016; Bajpai, 2017; Chen and Lee, 2018; Pereira and Arantes, 2018). Reddy and Rhim (2014) demonstrated that paper-mulberry (*Broussonetia kazinoki* Siebold) bast pulp could be used as a new, environmentally friendly nanocellulose source. Bettaieb et al. (2015a, 2015b) reported on the preparation of a new source of nanocellulose crystals extracted from *Posidonia oceanica* leaves and balls. Nanocellulose fibers with a high crystallinity index (CI) of about 70% and improved thermal stability were produced from pinecones (Jack pine: *Pinus banksiana* Lamb.) using chemical and mechanical treatments (Rambabu et al., 2016). Chen and Lee (2018) recently isolated nanocellulose from *Panax ginseng*, spent tea residue, waste cotton cloth, and old corrugated cardboard, and demonstrated its potential in commercial applications for sustainable development.

For the islands of the Macaronesia archipelagos (Azores (Portugal), Madeira (Portugal), Canary Islands (Spain), and Cape Verde) and other regions of the world, the revalorization of invasive plants such as *A. americana*, *A. donax* (giant reed), *Pennisetum setaceum*, and *Ricinus communis* for the production of biomaterials and composites would constitute an environmental benefit and an attractive economic income that would support eradication campaigns. The plants mentioned above are currently utilized only as a source of cellulose fibers for the textile and automobile industries (Ridzuan et al., 2016; Motaung et al., 2017; Trifol et al., 2017; Vinayaka et al., 2017). To the best of our knowledge, no attempts have been made to use the fibers of these invasive plant species as an inexpensive nanocellulose source for biomedical applications. In the present study, we chose the fast-growing, widely distributed, and highly abundant plants *A. americana* and *R. communis* to produce cytocompatible nanoscaled cellulose. The exploration and revalorization of these plants are particularly crucial for the Macaronesia archipelagos island, where they present a severe environmental problem since they occupy abandoned agricultural land and all areas not cared for or that have been victims of the fire. Therefore, the primary objective of the study was to explore the potential of the selected invasive plants as an inexpensive and abundantly available renewable source of natural, highly crystalline cellulose nanofibers.

2 Materials and methods

2.1 Materials

Two samples of invasive plants, *A. americana* and *R. communis*, were collected from the Macaronesia archipelago, specifically on Gran Canaria island (Canary Islands archipelago, Spain); plants were collected from abandoned farmland (global positioning system (GPS) coordinates: 28.079 766, −15.455 594) now transformed into the urban ground, and oven-dried for 24 h at 105 °C before further use.

All reagents were purchased from Sigma Aldrich (Madrid, Spain or Lisbon, Portugal) and were used without further purification.

2.2 Cellulose extraction procedure

Cellulose nanofibers were extracted from two different raw material sources, *A. americana* and *R. communis*. Before extraction, the raw, dried, and milled plants were processed by refluxing with toluene-ethanol (2:1, volume ratio) for 8 h in a Soxhlet apparatus to remove pigments, waxes, and lipids. The raw materials were then thoroughly washed on a Büchner funnel with ethanol, acetone, and distilled water, and dried at room temperature until a constant weight was achieved. Subsequently, two different methods were used for cellulose extraction, as presented in Fig. 1 and detailed below.

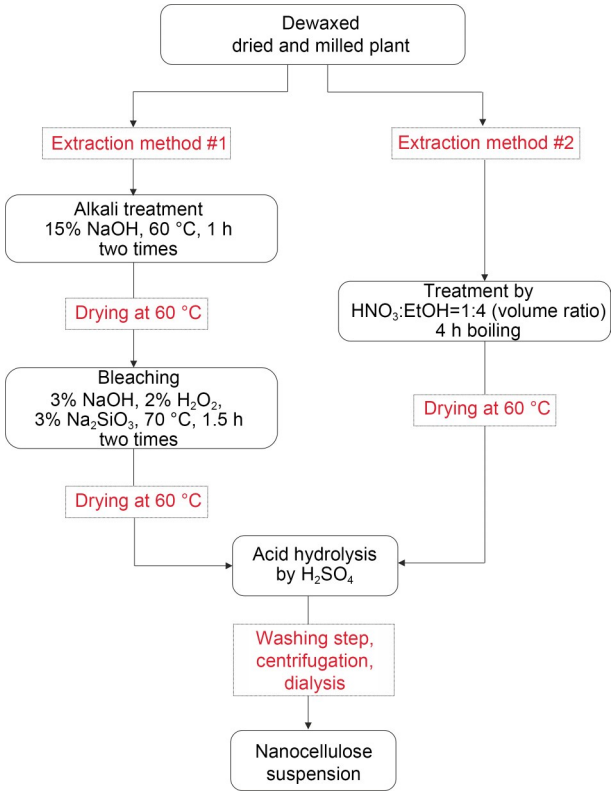

Fig. 1 Cellulose nanofiber extraction methods. The concentrations of 15% NaOH, 3% NaOH, 2% H_2O_2, and 3% Na_2SiO_3 are all at mass fractions.

2.2.1 Extraction method #1, based on an alkali treatment

The dewaxed dried samples were treated with 15% (mass fraction) of NaOH solution at 60 °C for 1 h under mechanical stirring, using a fiber to liquid ratio of 1:15. After filtration and extensive washing with distilled water on a Büchner funnel, the residue was dried at room temperature until a constant weight was achieved. The alkali-treated fibers were bleached with a mixture of 3% NaOH, 2% H_2O_2, and 3% Na_2SiO_3 (all at mass fraction) solution at 70 °C for 1.5 h under mechanical stirring using a fiber to liquid ratio of 1:60. This treatment was repeated twice. After bleaching, the fibers were thoroughly washed with distilled water until a neutral pH was obtained and then dried overnight until a constant weight was achieved. The prepared *A. americana* and *R. communis* fibers were mixed with a 60% (mass fraction, the same below) H_2SO_4 solution and stirred vigorously at 45 °C for 2.5 and 4.5 h, respectively. After that, hydrolysis was immediately quenched by adding 500 mL of cold distilled water to the reaction mixture. The resulting nanocellulose suspension was centrifuged several times (10 000 r/min, 10 min) to separate the nanocellulose from the sulphuric acid solution. The final suspension was continuously dialyzed (dialysis membrane 1000 Da) against distilled water to remove the sulfate ions until a constant, neutral pH was reached. Finally, the obtained nanocellulose suspension was freeze-dried and stored at 8 °C for further characterization.

2.2.2 Extraction method #2, based on acid hydrolysis

The dewaxed dried samples were pretreated using the Kurschner-Hoffer method (Béakou et al., 2008). The resulting sample was refluxed with a mixture of nitric acid and ethyl alcohol (1:4, volume ratio) for 4 h in total. The residue was filtered off and then refluxed again with the alcohol/nitric acid solution. This procedure was repeated three times. Finally, the residue was filtered off and washed with hot distilled water until a neutral pH was achieved. This was followed by drying in an oven at 60 °C until a constant weight was obtained. Then, the prepared *A. americana* fibers were mixed with a 40% H_2SO_4 solution and stirred vigorously at 60 °C for 2 h. *R. communis* fibers were mixed with a 60% H_2SO_4 solution and stirred vigorously at 45 °C for 2.5 h. The ratio of fibers to the acid solution was 1:40. After that, hydrolysis was immediately quenched by adding 500 mL of cold distilled water to the reaction mixture. Non-reactive sulfate groups were removed from the resulting suspension by centrifugation, separating the nanocellulose from the solution after each washing step. The final suspension was continuously dialyzed (dialysis membrane 1000 Da) against distilled water until a constant neutral pH was reached.

Finally, the obtained nanocellulose suspension was freeze-dried and stored at 8 °C for further characterization. The details of the extraction conditions for each prepared sample are provided in Table 1.

2.3 Characterization

2.3.1 Chemical composition of raw materials

The chemical composition of the raw materials was measured as follows: the lignin content was determined according to the Klason method based on an initial 72% H_2SO_4 hydrolysis step, followed by dilution with water to 3% H_2SO_4 and reflux boiling in the secondary hydrolysis step (Theander and Westerlund, 1986). The acid-insoluble residue (AIR) was calculated by the difference between the mass of the acid detergent-insoluble residue and the residual mass after the treatment. The presence of acid-soluble lignin (ASL) in the first filtrate was determined by ultraviolet-visible (UV-Vis) spectroscopy. Total cellulose content of the invasive species was investigated with the Kürschner-Hoffer method, which is based on the treatment of fibers with a mixture of nitric acid and ethanol (1:4, volume ratio) for a total duration of 4 h (Béakou et al., 2008). The hemicellulose content (C_h, %) was estimated theoretically as: C_h=100−C_c−C_l, where C_c is cellulose content (%) and C_l is lignin content (%). An average of three replicates was calculated for each sample.

2.3.2 Morphology analysis

The morphology of the obtained freeze-dried nanocellulose samples was characterized with a scanning electron microscope at an accelerating voltage of 15 kV (Analytical JEOL 7001F FEG-SEM, JEOL, Tokyo, Japan). All samples were sputter-coated with a thin layer of Au before observation. Additional scanning electron microscopy (SEM) images and the energy-dispersive X-ray spectroscopy (EDX) analysis of the raw materials were obtained on a desktop SEM Phenom-ProX (ThermoFisher Scientific, London, UK). Samples were observed in their natural state, i.e., without any coating, using a Phenom Charge Reduction Sample Holder (ThermoFisher Scientific).

The hydrodynamic diameter distribution and zeta potential of the obtained cellulose nanofibers were determined by dynamic light scattering (DLS) and electrophoretic light scattering (ELS), respectively, using a Zetasizer Nano ZS (Malvern Instruments Ltd., Malvern, UK) at 25 °C before the freeze-drying process. Three measurements were taken for each case; the mean value and standard deviation are reported.

2.3.3 X-ray diffraction and crystallinity studies

X-ray diffraction (XRD) studies of the raw materials and the freeze-dried cellulose nanofibers were carried out using a Bruker X8 advanced diffractometer (Bruker, Leipzig, Germany). Samples were scanned in the range of 5°−52° for 2θ with increments of 0.02° using CuKα radiation (λ=1.54 Å=0.154 nm). The CI of the samples was calculated by the Segal method (Gümüskaya et al., 2003): CI= (I_{200} − I_{am})/I_{200}×100%, where I_{200} gives the maximum intensity of the peak corresponding to the plane in the sample with Miller index of 200, and I_{am} represents the intensity of diffraction of the non-crystalline material taken at an angle of 2θ=18° in the valley between the peaks.

The crystallite size (L) perpendicular to the plane was obtained by the Scherrer equation (Poletto et al., 2014): L=0.94λ/βcosθ, where λ is the X-ray wavelength (0.1542 nm), β is the full width at half-maximum in radians, and θ is the Bragg angle in radians.

2.3.4 Fourier transform infrared spectroscopy

The Fourier transform infrared (FTIR) spectra of the freeze-dried cellulose nanofibers were analyzed using a Spectrum Two™ spectrophotometer (Perkin-Elmer, Massachusetts, USA). The spectra were obtained from KBr pellets containing the samples (measured between a wavenumber range of 4000 to 400 cm^{-1}) at a scan rate of 32 scans/min in the transmittance mode.

Table 1 Extraction conditions of nanocellulose samples

Sample name	Source	Extraction method	H_2SO_4 (%, mass fraction)	Temperature (°C)	Hydrolysis time (h)
CNF_{AA1}	*Agave americana*	Method #1	60	45	2.5
CNF_{AA2}	*A. americana*	Method #2	40	60	2.0
CNF_{RC1}	*Ricinus communis*	Method #1	60	45	4.5
CNF_{RC2}	*R. communis*	Method #2	60	45	2.5

CNF: cellulose nanofiber.

2.3.5 Cell viability assay

The cytotoxic effects of the CNF_{AA1}, CNF_{AA2}, CNF_{RC1}, and CNF_{RC2} samples on human embryonic kidney 293T (HEK293T) cells were evaluated by thiazolyl blue tetrazolium bromide (MTT) colorimetric assay, establishing a correlation between cell metabolic activity and the number of viable cells in culture. Cell viability, which was studied as a function of the nanofiber type and its concentration, was assessed after exposing cells to various samples for 48 h. MTT was purchased from Sigma-Aldrich (Lisbon, Portugal), and where applicable, was used without further purification. Collagen (collagen I rat tail protein), Dulbecco's modified Eagle's medium (DMEM)-high glucose, fetal bovine serum (FBS), and antibiotic-antimycotic (AbAm) were purchased from Gibco® (ThermoFisher Scientific), while analytical-grade dimethyl sulfoxide (DMSO) was purchased from ThermoFisher Scientific.

Prior to cell cultivation, a 96-well plate was pretreated with collagen (type I, 0.2 mg/mL in 0.25% (volume fraction) acetic acid). Thereafter, HEK293T cells (ATCC® CRL-3216™) were seeded in a 96-well plate at a density of 5×10^3 cells/well using 200 μL DMEM supplemented with 10% FBS and 1% AbAm solution. The cells were cultured for 24 h at 37 °C in a humidified 5% CO_2 atmosphere. At this stage, the cell culture medium in each well was replaced with 180 μL of fresh serum-containing DMEM, and the cells were subsequently exposed to 20 μL of each cellulose nanofiber. Here, a 5 mg/mL stock solution of the nanofiber was first prepared by suspending it in a 5% DMSO solution and then diluting it using filter-sterilized ultrapure water to different concentrations. Final concentrations of 0, 50, 100, 200, 250, 300, 400, and 500 μg/mL were tested for each cellulose nanofiber under investigation.

After 48 h of incubation at 37 °C in a humidified 5% CO_2 atmosphere, the cell culture medium in each well was removed and replaced with a solution made up of 180 μL serum-containing DMEM and 20 μL MTT (5 mg/mL). The cells were further incubated for 4 h at 37 °C in a humidified 5% CO_2 atmosphere. The resultant medium in each well was then removed, and 100 μL DMSO was added to each well. This was followed by gentle shaking of the plate to help dissolve the purple MTT formazan crystals. Finally, the absorbance of each well was measured using a microplate reader (model Victor3 1420, PerkinElmer, Massachusetts, USA); the reference wavelength was set at 630 nm, and the absorbance at 490 nm was recorded. Three separate cell viability assays were conducted, where in each case, three replicates were analyzed for each sample under investigation.

3 Results and discussion

3.1 Chemical composition of raw materials

Chemical composition analysis showed that raw dried *A. americana* is composed of (33.2±1.8)% cellulose, (9.0±0.8)% lignin, and (12.1±0.6)% hemicellulose (all at mass fraction). Raw dried *R. communis* is composed of (34.4±1.8)% cellulose, (18.1±2.2)% lignin, and (32.9±4.3)% hemicellulose. The obtained results are comparable to data reported for other common lignocellulosic materials (Phanthong et al., 2018). Nevertheless, it is important to mention that the chemical composition of the plants significantly depends on many different factors like geographic location, climate, harvesting, and the age of the plant, as well as the extraction process and experimental conditions.

3.2 Morphology characterization of the obtained samples

The surface morphologies of the dried milled plants of *A. americana* and *R. communis* were investigated by SEM in conjunction with EDX analysis (Figs. 2 and 3). As can be seen from Fig. 2a, SEM images of raw *A. americana* (raw_AA) showed two different morphologies. One part of the samples had a layered structure, while the other part formed a network of microfibrils tightly packed together and covered with some outer membranes. Closer examination of the raw_AA microfibrils revealed the diameter of the original fibril to be around 3 μm, with the ribbon-shaped fibrils having a spiral appearance.

EDX analysis studies also revealed a homogeneous elemental composition throughout the whole fiber region, with several minerals commonly found in soil being identified (e.g., potassium and calcium; Fig. S1). The sample was very beam-sensitive, and the fibers were ultimately melted down and destroyed by the EDX electron beam.

Fig. 3a illustrates the morphology of the raw *R. communis* samples (raw_RC). It is evident that the structure consists of spiral-shaped microfibrils covered

with some non-cellulosic constituents (hemicellulose and lignin) (Sair et al., 2017).

Nanocellulose isolation was performed using the two different processes described above. Figs. 2b and 2c and Figs. 3b and 3c show the SEM micrographs of the freeze-dried cellulose nanofibers extracted from *A. americana* and *R. communis* fibers, respectively. The results indicated that both extraction methods contributed to structural changes in the cellulose nanofibers compared with the raw fibers. All synthesized samples exhibited a uniform and smooth morphology. We found that samples CNF_{AA1} and CNF_{RC1} extracted by method #1 had needle-shaped structures (Figs. 2b and 3b).

On the other hand, the CNF_{AA2} and CNF_{RC2} samples extracted by method #2 (based on sequential acid hydrolysis) showed a network with a structured fibrous morphology (Figs. 2c and 3c). One of the main advantages of method #2 lies in the simplicity of the process since the application of the Kürschner-Hoffer method entails a rapid pre-treatment step for sample purification to remove the non-cellulosic components. The size distribution of the prepared samples measured by DLS is shown in Fig. S2. The cellulose nanofibers of the CNF_{AA1} and CNF_{AA2} samples had an average diameter of 58 and 141 nm, respectively, while the diameters of CNF_{RC1} and CNF_{RC2}

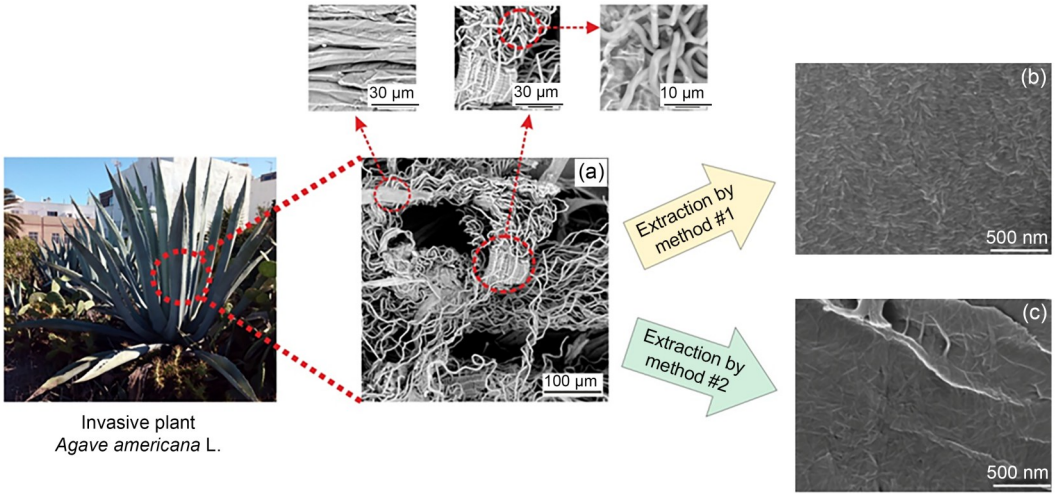

Fig. 2 Scanning electron microscopy (SEM) images of the raw *Agave americana* (raw_AA) (a) and cellulose nanofibers extracted from *A. americana* by extraction method #1 (CNF_{AA1}) (b) and extraction method #2 (CNF_{AA2}) (c).

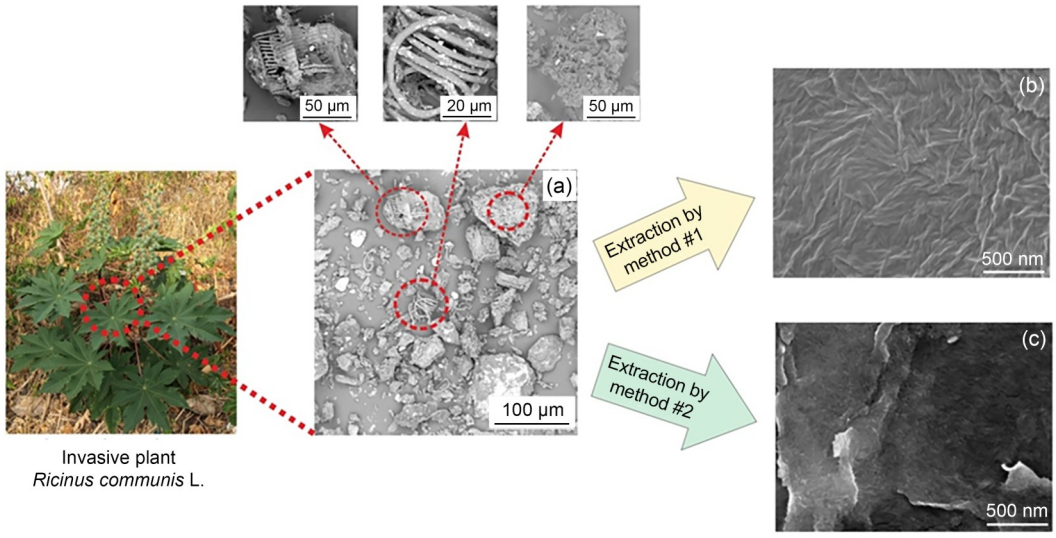

Fig. 3 Scanning electron microscopy (SEM) images of the raw *Ricinus communis* (raw_RC) (a) and cellulose nanofibers extracted from *R. communis* by extraction method #1 (CNF_{RC1}) (b) and extraction method #2 (CNF_{RC2}) (c).

were about 68 and 120 nm, respectively. As expected, the obtained average hydrodynamic size for all samples incorporated water in the primary hydration layers.

3.3 XRD characterization

The XRD results of the raw fibers and the extracted cellulose nanofibers are presented in Figs. 4 and 5 and Table 2.

It should be noted that the structure and CI of the obtained samples depended on both the raw source of cellulose and the chemical extraction method applied. The raw *A. americana* fibers (i.e., raw_AA) and the cellulose nanofibers isolated from them had a crystalline nature (Fig. 4). The raw_AA sample, in particular, displayed typical cellulose I structure with characteristic diffraction peaks at 2θ=16.4°, 22.6°, and 34.5°, indexed as (110), (200), and (004) planes, respectively (Fig. 4).

The application of method #1 for CNF_{AA1} extraction from *Agave* fibers led to a change in the crystal form of the native cellulose I (Fig. 4). The CNF_{AA1} sample was a mixture of cellulose types I and II, as can be observed from the appearance of two peaks at 2θ=20.0° (110) and 22.0° (020), instead of the one main peak at 22.6°. The obtained results were in agreement with previous studies (le Moigne and Navard, 2010; Sghaier et al., 2012). In particular, Sghaier et al. (2012) reported a transformation of the crystal structure of *A. americana* fibers from cellulose I to cellulose II caused by mercerisation with NaOH, while bleaching with NaOCl treatment had no crucial effect on the *Agave* fiber properties. On the other hand, the CNF_{AA2} sample isolated by method #2 had a similar diffraction pattern to that of the raw *Agave* fibers (Fig. 4). For this sample, the 2θ peaks were observed at 16.0° (110), 22.8° (200), and 34.5° (004), corresponding to the cellulose structure type I. For the *A. americana* fibers, both extraction methods contributed to a significant decrease in the amount of amorphous content in the samples. Nevertheless, as shown by the data reported in Table 2, the chemical treatment of the raw *Agave* fibers by method #2 significantly increased the CI of the cellulose nanofibers compared to extraction method #1. The calculated CIs of the raw_AA, CNF_{AA1}, and CNF_{AA2} samples were found to be 70.4%, 87.7%, and 94.1%, respectively. Das et al. (2010) obtained crystallinity values of 66.5% for cotton nanofibers and 78.0% for jute, with crystallite sizes of 2.58 and 3.68 nm, respectively (perpendicular to the 101 plane); nanocrystalline cellulose obtained by acid hydrolysis from newspapers reached a CI of up to 90.2%, with a crystallite size of 5.7 nm (Mohamed et al., 2015). The average crystallite size was calculated using the Scherrer formula. Estimation of the sizes of raw_AA, CNF_{AA1}, and CNF_{AA2} resulted in values of 2.5, 4.6, and 3.9 nm, respectively.

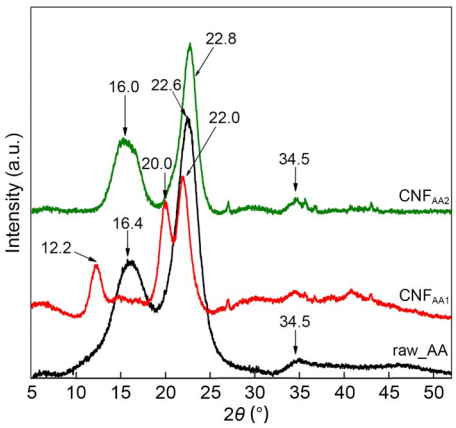

Fig. 4 X-ray diffraction (XRD) patterns of the cellulose nanofibers obtained from *Agave americana*: raw *A. americana* (raw_AA), CNF_{AA1}, and CNF_{AA2}.

Table 2 X-ray diffraction (XRD) data and crystallinity parameters

Plane	Cellulose polymorph	2θ (°)					
		Raw_AA	CNF_{AA1}	CNF_{AA2}	Raw_RC	CNF_{RC1}	CNF_{RC2}
(1-10)	Cellulose II		12.2				12.0
(1-10)	Cellulose I						15.0
(110)	Cellulose I	16.4		16.0		16.0	16.4
(110)	Cellulose I		20.0				
(112)	Cellulose II						20.2
(020)	Cellulose II		22.0				
(200)	Cellulose I	22.6		22.8	22.0	22.6	22.6
(004)	Celluloses I and II	34.5	34.5	34.5		34.7	34.0
Crystallinity index (%)		70.4	87.7	94.1		90.7	92.7
Crystallite size (nm)		2.5	4.6	3.9		3.4	4.6

The X-ray diffraction patterns of the raw_RC, CNF_{RC1}, and CNF_{RC2} samples are presented in Fig. 5. As can be seen, the diffraction pattern of raw *R. communis* fibers (i.e., raw_RC) is dominated by a broad, amorphous halo, showing a broad peak at around 22.0° in the (200) plane, typical for cellulose type I (Fig. 5). The X-ray diffraction diagram of CNF_{RC1} showed three characteristic peaks at 16.0° (110), 22.6° (200), and 34.7° (004), typical of the cellulose I structure (Fig. 5). Compared to CNF_{AA2}, the pattern of the CNF_{RC2} sample extracted using method #2 exhibited peaks at 2θ=12.0° (1−10), 15.0° (1−10), 16.4° (110), 20.2° (112), 22.6° (200), and 34.0° (004), indicating a mixture of the cellulose types I and II crystal structures (Fig. 5). Nanocrystalline cellulose from cotton shows characteristics peaks at around 15.0° (110) and 23.0° (200), similar to what is observed here. Peaks at 2θ=14.8°, 16.4°, 22.6°, and 34.6° are typical of cellulose I, while the one at 22.6° indicates a higher perfection of the crystal structure in the (200) plane (Mohamed et al., 2015); this peak is found for samples with higher crystallinity values. The CI value of CNF_{RC1} was found to be 90.7%. After extraction by method #2, the CI of CNF_{RC2} was slightly higher (i.e., 92.7%). Estimation of the sizes of CNF_{RC1} and CNF_{RC2} resulted in values of 3.4 and 4.6 nm, respectively.

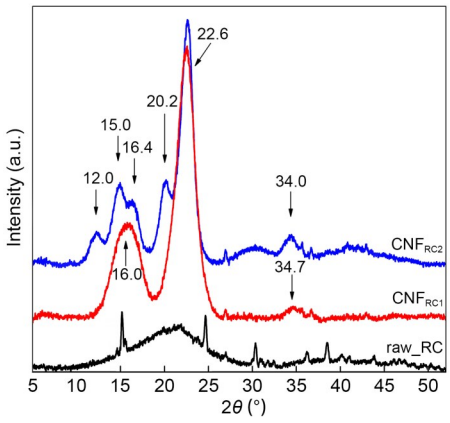

Fig. 5 X-ray diffraction (XRD) patterns of the cellulose nanofibers obtained from *Ricinus communis*: raw *R. communis* (raw_RC), CNF_{RC1}, and CNF_{RC2}.

These results showed that for both *A. americana* and *R. communis* fibers, extraction method #2 was better at producing highly crystalline cellulose nanofibers once ethanol at high temperatures had dissolved lignin and nitric acid had destroyed hemicellulose.

3.4 FTIR spectroscopy

The FTIR spectra of the CNF_{AA1}, CNF_{AA2}, CNF_{RC1}, and CNF_{RC2} samples are presented in Fig. 6. The broad band positioned in the 3600–3000 cm^{-1} region was observed in all the synthesized cellulose fiber samples and indicates the O–H stretching vibrations of the hydrogen-bonded hydroxyl group in the cellulose molecules involved in intermolecular hydrogen bonds (Poletto et al., 2014). The absorption peak at 1642 cm^{-1} in all the synthesized samples indicates the presence of water, due to the presence of O–H bending. Although all the FTIR samples were freeze-dried before analysis, it was difficult to completely eliminate water from the cellulose molecules due to the strong cellulose−water interactions. One of the possible explanations is that the open surfaces created in the nanocellulose by the removal of lignin and hemicellulose helped in the absorption of moisture, leading to higher moisture content (Lam et al., 2012). The presence of the absorption peak at 2900 cm^{-1} can be attributed to the stretching vibrations of the C−H groups of cellulose (Bettaieb et al., 2015a). The absorption peak in the spectrum near 1159 cm^{-1} is attributable to the C−O−C asymmetric stretching vibrations of cellulose. Several characteristic absorption bands showed that there were differences in the chemical structure of the cellulose nanofiber samples obtained by the two different extraction methods. This was the case for CNF_{AA1} and CNF_{RC1} samples isolated by method #1. The weak shoulders at 2854 cm^{-1} or/and 1740 cm^{-1} in the FTIR spectra are indicative of the presence of lignin content. In the case of the CNF_{AA2} and CNF_{RC2} samples isolated by method #2, these peaks were not detected. The band around 897 cm^{-1} is associated with an

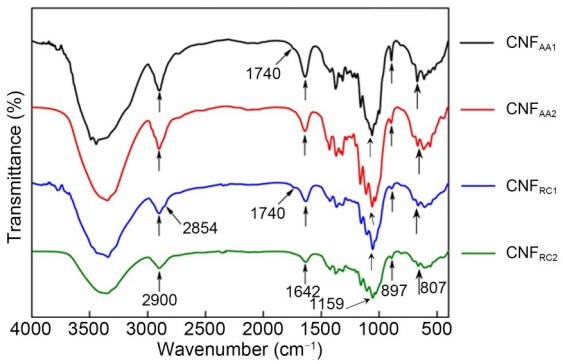

Fig. 6 Fourier transform infrared (FTIR) spectra of cellulose nanofibers obtained from *Agave americana* and *Ricinus communis*.

amorphous region in cellulose (Hospodarova et al., 2018) (β-glycosidic linkages (Mohamed et al., 2015)), which seems to be less important for *R. communis* samples and for *Agave* treated under method #2, which is in accordance with the results from crystallinity measures shown in Table 2. For all the synthesized samples, the presence of the symmetrical C−O−S vibration at 807 cm^{-1} is associated with the C−O−SO_3 groups. This result was confirmed by zeta potential measurements, where the negative ζ-potential values obtained for the CNF_{AA1}, CNF_{AA2}, CNF_{RC1}, and CNF_{RC2} samples can be explained by the presence of the negatively charged sulfate groups on the nanocellulose surface (Table S1).

3.5 Cytotoxicity assays

Cytotoxicity is an important issue that needs to be addressed before using any chemical compound or material on humans. Since the *A. americana* and *R. communis* cellulose nanofibers prepared in this study may be considered for future use in biomedical applications, their cytocompatibility with human cells was evaluated. As can be seen in Fig. 7, the cellulose nanofibers obtained using both extraction methods were all cytocompatible, as the HEK293T cells showed good viability. In the case of the cellulose nanofibers obtained using extraction method #1 (i.e., CNF_{AA1} and CNF_{RC1}), the exposed cells were capable of actively metabolizing MTT in the concentration range assayed (i.e., 0−500 μg/mL). For the nanofibers obtained using extraction method #2 (i.e., CNF_{AA2} and CNF_{RC2}), the cells were also observed to actively metabolize MTT in the same concentration range, but to a lesser extent relative to their method #1 counterparts (i.e., CNF_{AA1} and CNF_{RC1}); this may be related to the crystallinity (it seems that the higher the CI, the lower the MTT metabolization). Moreover, relative to the CNF_{AA1}, CNF_{RC1}, and CNF_{RC2} samples, only the CNF_{AA2} sample was observed to exert a mild cytotoxic effect on the HEK293T cells when using a sample concentration of 500 μg/mL (<80% cell metabolic activity).

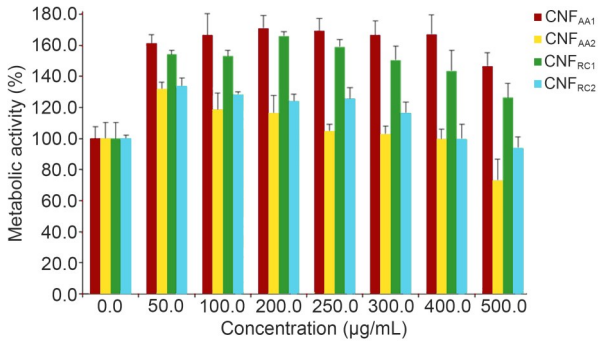

Fig. 7 Thiazoyl blue tetrazolium bromide (MTT) viability assay of HEK293T cells treated with cellulose nanofibers derived from *Agave americana* and *Ricinus communis*. Increasing concentrations of the CNF_{AA1}, CNF_{AA2}, CNF_{RC1}, and CNF_{RC2} samples were used to treat the cells for 48 h after cell seeding. All results are expressed as the mean± standard deviation (SD), with n=3.

Interestingly, cell viability was shown to be higher than the control values in most situations, which likely reflects a release of glucose from the nanofibers over time and its use in cell metabolism. Overall, *A. americana* and *R. communis* cellulose nanofibers prepared in this study were shown to be cytocompatible, with the potential to be used for future biomedical applications.

4 Conclusions

The fibers of invasive species *A. americana* and *R. communis* can be successfully used as a new source to produce very highly crystalline cellulose nanofibers with a CI of 94.1% and 92.7%, respectively, by two different processes, based on a first step of alkaline or acid treatment. The nanofibers produced by both methods are also cytocompatible in the concentration range tested (0−500 μg/mL) on HEK293T cells. In conclusion, this work demonstrates that not only can nanocellulose be extracted from the fibers of these two species of invasive plants, but also it has high intrinsic potential as a new renewable green source of highly crystalline cellulose-based nanomaterials for biomedical applications.

Acknowledgments

The authors acknowledge the Programa de Cooperación Territorial INTERREG V-A MAC 2014-2020 and Inv2Mac Project (MAC/4.6d/229), as well as the partial support of FCT-Fundação para a Ciência e a Tecnologia (Base Fund UIDB/00674/2020). ARDITI-Agência Regional para o Desenvolvimento da Investigação Tecnologia e Inovação supported the study through the project M1420-01-0145-FEDER-000005-CQM$^+$ (Madeira 14-20 Program); the Post-doc Grant (M1420-09-5369-FSE-000001, 002458/2015/132) for Carla S. ALVES is also acknowledged.

Author contributions

Experiments, data analysis, and original draft preparation: Olga L. EVDOKIMOVA; experiments, data analysis, and writing the manuscript: Carla S. ALVES and Radenka M. KRSMANOVIĆ WHIFFEN; experiments, data analysis, funding acquisition, resources, and writing and editing the manuscript: Zaida ORTEGA; data analysis, and writing and editing the manuscript: Helena TOMÁS; conceptualization, supervision, funding acquisition, resources, data analysis, and writing and editing the manuscript: João RODRIGUES. All authors have read and agreed to the published version of the manuscript. The authors have full access to all the data in the study and take responsibility for the integrity and security of the data.

Compliance with ethics guidelines

Olga L. EVDOKIMOVA, Carla S. ALVES, Radenka M. KRSMANOVIĆ WHIFFEN, Zaida ORTEGA, Helena TOMÁS, and João RODRIGUES declare that they have no conflict of interest.

This article does not contain any studies with human or animal subjects performed by any of the authors.

References

Abrantes S, Amaral ME, Costa AP, et al., 2007. *Cynara cardunculus* L. alkaline pulps: alternatives fibres for paper and paperboard production. *Bioresour Technol*, 98(15): 2873-2878. https://doi.org/10.1016/j.biortech.2006.09.052

Aguir C, M'Henni MF, 2006. Experimental study on carboxymethylation of cellulose extracted from *Posidonia oceanica*. *J Appl Polym Sci*, 99(4):1808-1816. https://doi.org/10.1002/app.22713

Åhlén M, Tummala GK, Mihranyan A, 2018. Nanoparticle-loaded hydrogels as a pathway for enzyme-triggered drug release in ophthalmic applications. *Int J Pharm*, 536(1):73-81. https://doi.org/10.1016/j.ijpharm.2017.11.053

Bacakova L, Pajorova J, Bacakova M, et al., 2019. Versatile application of nanocellulose: from industry to skin tissue engineering and wound healing. *Nanomaterials (Basel)*, 9(2):164. https://doi.org/10.3390/nano9020164

Bajpai P, 2017. Pulp and Paper Industry. Elsevier, Amsterdam, p.15-25. https://doi.org/10.1016/b978-0-12-811101-7.00002-2

Béakou A, Ntenga R, Lepetit J, et al., 2008. Physico-chemical and microstructural characterization of "*Rhectophyllum camerunense*" plant fiber. *Compos Part A: Appl Sci Manuf*, 39(1):67-74. https://doi.org/10.1016/j.compositesa.2007.09.002

Bettaieb F, Khiari R, Dufresne A, et al., 2015a. Mechanical and thermal properties of *Posidonia oceanica* cellulose nanocrystal reinforced polymer. *Carbohydr Polym*, 123: 99-104. https://doi.org/10.1016/j.carbpol.2015.01.026

Bettaieb F, Khiari R, Hassan ML, et al., 2015b. Preparation and characterization of new cellulose nanocrystals from marine biomass *Posidonia oceanica*. *Ind Crops Prod*, 72: 175-182. https://doi.org/10.1016/j.indcrop.2014.12.038

Charles H, Dukes JS, 2007. Impacts of invasive species on ecosystem services. *In*: Nentwig W (Ed.), Biological Invasions. Springer, Heidelberg, p.217-237. https://doi.org/10.1007/978-3-540-36920-2_13

Chen YW, Lee HV, 2018. Revalorization of selected municipal solid wastes as new precursors of "green" nanocellulose via a novel one-pot isolation system: a source perspective. *Int J Biol Macromol*, 107:78-92. https://doi.org/10.1016/j.ijbiomac.2017.08.143

Crowl TA, Crist TO, Parmenter RR, et al., 2008. The spread of invasive species and infectious disease as drivers of ecosystem change. *Front Ecol Environ*, 6(5):238-246. https://doi.org/10.1890/070151

Das K, Ray D, Bandyopadhyay NR, et al., 2010. Study of the properties of microcrystalline cellulose particles from different renewable resources by XRD, FTIR, nanoindentation, TGA and SEM. *J Polym Environ*, 18(3):355-363. https://doi.org/10.1007/s10924-010-0167-2

Fiore V, Scalici T, Vitale G, et al., 2014. Static and dynamic mechanical properties of *Arundo Donax* fillers-epoxy composites. *Mater Des*, 57:456-464. https://doi.org/10.1016/j.matdes.2014.01.025

Fiserova M, Gigac J, Majtnerova A, et al., 2006. Evaluation of annual plants (*Amaranthus caudatus* L., *Atriplex hortensis* L., *Helianthus tuberosus* L.) for pulp production. *Cellul Chem Technol*, 40(6):405-412.

Guise C, Fangueiro R, 2016. Biomedical applications of nanocellulose. *In*: Fangueiro R, Rana S (Eds.), Natural Fibres: Advances in Science and Technology Towards Industrial Applications. Springer, Dordrecht, p.155-169. https://doi.org/10.1007/978-94-017-7515-1_12

Gümüskaya E, Usta M, Kirci H, 2003. The effects of various pulping conditions on crystalline structure of cellulose in cotton linters. *Polym Degrad Stab*, 81(3):559-564. https://doi.org/10.1016/S0141-3910(03)00157-5

Hospodarova V, Singovszka E, Stevulova N, 2018. Characterization of cellulosic fibers by FTIR spectroscopy for their further implementation to building materials. *Am J Anal Chem*, 9(6):303-310. https://doi.org/10.4236/ajac.2018.96023

Kargarzadeh H, Ioelovich M, Ahmad I, et al., 2017. Methods for extraction of nanocellulose from various sources. *In*: Kargarzadeh H, Ahmad I, Thomas S, et al. (Eds.), Handbook of Nanocellulose and Cellulose Nanocomposites,

Volume 1. Wiley-VCH Verlag GmbH & Co. KGaA, Weinheim, p.1-49. https://doi.org/10.1002/9783527689972.ch1

Khiari R, Mauret E, Belgacem MN, et al., 2011. Tunisian date palm rachis used as an alternative source of fibres for papermaking applications. *BioResources*, 6(1):265-281.

Lam E, Male KB, Chong JH, et al., 2012. Applications of functionalized and nanoparticle-modified nanocrystalline cellulose. *Trends Biotechnol*, 30(5):283-290. https://doi.org/10.1016/j.tibtech.2012.02.001

Lang N, Merkel E, Fuchs F, et al., 2015. Bacterial nanocellulose as a new patch material for closure of ventricular septal defects in a pig model. *Eur J Cardio-Thorac Surg*, 47(6):1013-1021. https://doi.org/10.1093/ejcts/ezu292

le Moigne N, Navard P, 2010. Dissolution mechanisms of wood cellulose fibres in NaOH-water. *Cellulose*, 17(1):31-45. https://doi.org/10.1007/s10570-009-9370-5

Lin N, Dufresne A, 2014. Nanocellulose in biomedicine: current status and future prospect. *Eur Polym J*, 59:302-325. https://doi.org/10.1016/j.eurpolymj.2014.07.025

Maheswari CU, Reddy KO, Muzenda E, et al., 2012. Extraction and characterization of cellulose microfibrils from agricultural residue—*Cocos nucifera* L. *Biomass Bioenergy*, 46:555-563. https://doi.org/10.1016/j.biombioe.2012.06.039

Mishra RK, Sabu A, Tiwari SK, 2018. Materials chemistry and the futurist eco-friendly applications of nanocellulose: status and prospect. *J Saudi Chem Soc*, 22(8):949-978. https://doi.org/10.1016/j.jscs.2018.02.005

Mohamed MA, Salleh WNW, Jaafar J, et al., 2015. Physicochemical properties of "green" nanocrystalline cellulose isolated from recycled newspaper. *RSC Adv*, 5(38): 29842-29849. https://doi.org/10.1039/c4ra17020B

Mooney HA, Hobbs RJ, 2000. Invasive Species in a Changing World. Islands Press, p.65-73. https://islandpress.org/books/invasive-species-changing-world

Motaung TE, Linganiso LZ, Kumar R, et al., 2017. Agave and sisal fibre-reinforced polyfurfuryl alcohol composites. *J Thermoplastic Compos Mater*, 30(10):1323-1343. https://doi.org/10.1177/0892705716632858.

Ortega Z, Castellano J, Suárez L, et al., 2019. Characterization of *Agave americana* L. plant as potential source of fibres for composites obtaining. *SN Appl Sci*, 1:987. https://doi.org/10.1007/s42452-019-1022-2

Oun AA, Rhim JW, 2016. Characterization of nanocelluloses isolated from Ushar (*Calotropis procera*) seed fiber: effect of isolation method. *Mater Lett*, 168:146-150. https://doi.org/10.1016/j.matlet.2016.01.052

Pereira B, Arantes V, 2018. Nanocelluloses from sugarcane biomass. *In*: Chandel AK, Silveira MHL (Eds.), Advances in Sugarcane Biorefinery: Technologies, Commercialization, Policy Issues and Paradigm Shift for Bioethanol and By-Products. Elsevier Inc., Amsterdam, p.179-196. https://doi.org/10.1016/B978-0-12-804534-3.00009-4

Phanthong P, Reubroycharoen P, Hao XG, et al., 2018. Nanocellulose: extraction and application. *Carbon Res Convers*, 1(1):32-43. https://doi.org/10.1016/j.crcon.2018.05.004

Poletto M, Ornaghi HL, Zattera AJ, 2014. Native cellulose: structure, characterization and thermal properties. *Materials (Basel)*, 7(9):6105-6119. https://doi.org/10.3390/ma7096105

Rambabu N, Panthapulakkal S, Sain M, et al., 2016. Production of nanocellulose fibers from pinecone biomass: evaluation and optimization of chemical and mechanical treatment conditions on mechanical properties of nanocellulose films. *Ind Crops Prod*, 83:746-754. https://doi.org/10.1016/j.indcrop.2015.11.083

Reddy JP, Rhim JW, 2014. Characterization of bionanocomposite films prepared with agar and paper-mulberry pulp nanocellulose. *Carbohydr Polym*, 110:480-488. https://doi.org/10.1016/j.carbpol.2014.04.056

Rees A, Powell LC, Chinga-Carrasco G, et al., 2015. 3D bioprinting of carboxymethylated-periodate oxidized nanocellulose constructs for wound dressing applications. *BioMed Res Int*, 2015:925757. https://doi.org/10.1155/2015/925757

Ridzuan MJM, Majid MSA, Afendi M, et al., 2016. Characterisation of natural cellulosic fibre from *Pennisetum purpureum* stem as potential reinforcement of polymer composites. *Mater Des*, 89:839-847. https://doi.org/10.1016/j.matdes.2015.10.052

Sair S, Oushabi A, Kammouni A, et al., 2017. Effect of surface modification on morphological, mechanical and thermal conductivity of hemp fiber: characterization of the interface of hemp–polyurethane composite. *Case Stud Therm Eng*, 10:550-559. https://doi.org/10.1016/j.csite.2017.10.012

Sandler N, Preis M, 2016. Printed drug-delivery systems for improved patient treatment. *Trends Pharmacol Sci*, 37(12):1070-1080. https://doi.org/10.1016/j.tips.2016.10.002

Satyanarayana KG, Flores-Sahagun THS, Santos LPD, et al., 2013. Characterization of blue agave bagasse fibers of Mexico. *Compos Part A: Appl Sci Manuf*, 45:153-161. https://doi.org/10.1016/j.compositesa.2012.09.001

Sghaier AEOB, Chaabouni Y, Msahli S, et al., 2012. Morphological and crystalline characterization of NaOH and NaOCl treated *Agave americana* L. fiber. *Ind Crops Prod*, 36(1):257-266. https://doi.org/10.1016/j.indcrop.2011.09.012

Sun DY, Onyianta AJ, O'Rourke D, et al., 2020. A process for

deriving high quality cellulose nanofibrils from water hyacinth invasive species. *Cellulose*, 27(7):3727-3740. https://doi.org/10.1007/s10570-020-03038-4

Theander O, Westerlund EA, 1986. Studies on dietary fiber. 3. Improved procedures for analysis of dietary fiber. *J Agric Food Chem*, 34(2):330-336. https://doi.org/10.1021/jf00068a045

Trifol J, Sillard C, Plackett D, et al., 2017. Chemically extracted nanocellulose from sisal fibres by a simple and industrially relevant process. *Cellulose*, 24(1):107-118. https://doi.org/10.1007/s10570-016-1097-5

Vinayaka DL, Guna V, Madhavi D, et al., 2017. *Ricinus communis* plant residues as a source for natural cellulose fibers potentially exploitable in polymer composites. *Ind Crops Prod*, 100:126-131. https://doi.org/10.1016/j.indcrop.2017.02.019

Wang XJ, Cheng F, Liu J, et al., 2016. Biocomposites of copper-containing mesoporous bioactive glass and nanofibrillated cellulose: biocompatibility and angiogenic promotion in chronic wound healing application. *Acta Biomater*, 46:286-298. https://doi.org/10.1016/j.actbio.2016.09.021

Xu WY, Wang XJ, Sandler N, et al., 2018. Three-dimensional printing of wood-derived biopolymers: a review focused on biomedical applications. *ACS Sustain Chem Eng*, 6(5):5663-5680. https://doi.org/10.1021/acssuschemeng.7b03924

Yu DG, Branford-White C, Ma ZH, et al., 2009. Novel drug delivery devices for providing linear release profiles fabricated by 3DP. *Int J Pharm*, 370(1-2):160-166. https://doi.org/10.1016/j.ijpharm.2008.12.008

Supplementary information

Figs. S1 and S2; Table S1